J Mol Model (2003) 9:379–389
DOI 10.1007/s00894-003-0159-4

ORIGINAL PAPER

Yong Chen · Chwen-Yang Shew

Theoretical studies of the conformational behavior of chain molecules containing polar groups: simulations of a poly(vinylidene fluoride) model

Received: 3 February 2003 / Accepted: 17 June 2003 / Published online: 27 September 2003

Abstract Atomistic Monte Carlo simulations have been conducted to elucidate the conformational behavior of a single chain molecule containing polar functional groups. Here, we resort to an atomistic poly(vinylidene fluoride) (PVDF) chain model as a representative example. The model is modified in such a way that bond lengths and bond angles are fixed, aiming to manifest the role of dipolar interactions. For a given chain length, chain conformation is sensitive to two environmental parameters, temperature and dielectric constant. The mean chain size increases when temperature and/or dielectric constant are increased. The conformational behavior is further characterized by chain size distribution function, and our findings show that temperature induced conformational transition for a chain molecule can be discrete or continuous, depending on its chain length. Also, the dipolar interactions in PVDF are effectively attractive, and enhance chain contraction. As a result, when the strength of dipolar interactions is increased, the discrete conformational transition shifts toward longer chains; and for a given chain length, such a transition occurs at higher temperatures.

Keywords Chain molecule · Dipolar interactions · Conformational transition

Introduction and background

Polar bonds are commonly found in a variety of polymer molecules, and play a crucial role in determining the chain conformation of biological macromolecules, such as proteins consisting of polar groups and/or hydrogen bonding [1]. Our understanding of the properties of biopolymers, such as protein folding, is hampered by their heterogeneous compositions and the multiple length-scaled interactions. Unlike most biopolymers, synthetic polymers may have regular chemical compositions. With careful design, some synthetic polymers can serve as model systems and enable us to elucidate the influences of molecular interactions on chain conformations. From the standpoint of theoretical models, polymers containing strong polar bonds are between the limiting cases of neutral and fully-charged ionic polymers. However, the effects of electrostatic dipolar interactions arising from the strong polymer polar bonds on chain conformation have received less attention.

Several recent theoretical and experimental studies have involved chain-length dependent conformational behavior, which are related to protein folding problems. In the theoretical studies, short coarse-grained chain models (containing 3–30 monomers) were chosen, in which monomers, without detailed chemical structure, interact through simplified potentials such as square-well and Lennard-Jones potentials [2, 3]. Since the simulations involving strong attractive interactions are more difficult, such coarse-grained level models can be employed to increase computational efficiency and statistical accuracy, and provide the fundamental insights into complex polymer systems. Experimentally, short peptides have been designed in finding a critical chain length to form a specific secondary structure [4]. Also, the folding process of a short peptide, consisting of 20 amino acids, has been characterized [5], and will be used to test theoretical predictions obtained from molecular modeling rigorously. Inspired by these studies, we here utilize Monte Carlo (MC) simulation to investigate a model chain molecule containing polar bonds to address the issues regarding the chain conformational behavior under different environmental conditions, including temperature and dielectric constant, and for different chain lengths.

Among synthetic polymers, poly(vinylidene fluoride) (PVDF) is known to contain pronounced polar bonds. It has a regular chemical structure with methylene and fluoro-methylene groups alternating on the chain back-

Y. Chen · C.-Y. Shew (✉)
Department of Chemistry,
College of Staten Island of the City University of New York,
2800 Victory Boulevard, Staten Island, NY 10314, USA
e-mail: shew@postbox.csi.cuny.edu
Tel.: +1 718 982-3898
Fax: +1 718 982-3910

bone. In addition to standard molecular interaction potentials (vibrational energy, bending energy, nonbonded energy, and torsional energy), the recently developed molecular models consist of empirically modified atomic partial charges to account for strong dipolar interactions in a PVDF molecule [6, 7]. In our view, PVDF can be an ideal system to examine the general conformational behavior of polymer chains containing polar groups.

Recently, two PVDF molecular models have been devised [6, 7]. Karasawa and coworkers first developed molecular modeling through quantum calculations to investigate the properties of crystalline PVDF [6]. Byutner and Smith have extended this study to develop a more generalized molecular model for PVDF, applicable to different condensed phases, by using high level quantum mechanics calculations along with empirical modifications to improve the accuracy of the force field [7]. To test the force field, they conducted molecular dynamics simulations for short chain molecules. The bulk material density and chain characteristic ratio were extracted through extrapolation procedures, and the results by Byutner and Smith showed good agreement with experimental results for bulk amorphous polymeric materials of 1,000 monomers per chain [8]. Despite the success of the model, detailed chain properties, such as chain conformation, have not been investigated.

Since the vibrational and bending energy are not so crucial for chain conformational behavior, we modify the model by Byutner and Smith to fix the bond length and angle in our calculations. We employ Monte Carlo (MC) simulation to investigate the chain conformation of this simplified model because dipolar interactions are effectively attractive and may cause the chain to collapse. Compared to molecular dynamics simulations, MC simulations are a better approach to deal with systems trapped in local energy minima arising from attractive interactions [9], because more drastic moves can be implemented into MC simulations to force the chain molecule to cross the local energy barriers of metastable conformations [10, 11, 12].

To characterize chain conformational behavior, mean chain size and chain size distribution are the two widely used statistical properties. The latter property has been exploited to identify the complex conformational transition experimentally and theoretically [13, 14, 15, 16, 17], because the distribution function is directly related to the free energy as a function of chain size. With this property, Yamasaki and Yoshikawa found the discontinuous (sudden) conformational transition of DNA [13]. Near the transition point, the chain size distribution makes the transition from a single-modal to a bimodal function due to the coexistent globular and coiled conformational states, corresponding to two thermodynamic states.

In this work, we carry out atomistic Monte Carlo simulations to investigate the conformational behavior of a modified PVDF model in which bond lengths and bond angles are fixed. The simulation is conducted at the single chain level, and the condensed phase environment is treated as a dielectric continuum (for instance a single polymer in solvents or a tagged polymer in bulk materials). Such a model with explicit polar bonds and more realistic molecular interactions incorporated is beyond coarse-grained chain models. In the calculations, we use the environmental parameters, temperature and dielectric constant, to tune the strength of interaction potentials. The temperature is varied to change the strength of overall molecular interactions, while the dielectric constant is varied to adjust the strength of electrostatic interactions. In the simulations, we first test the simulation algorithm, and then calculate mean chain size and chain size distribution for different chain lengths, temperatures and dielectric constants. The chain-length dependent conformational transition is summarized in a schematic phase diagram in terms of temperature and chain length. To further verify the observed conformational transition, we expand the chain size distribution as a function of chain size and the corresponding conformation energy to correlate the chain size with conformational energy. In addition to temperature and chain length, the effects of polar bonds on chain conformation are drawn from these studies.

Model

In this work, we choose the all-atom force field developed by Byutner and Smith [7] to investigate the conformational transition of a PVDF molecule. Since bond length and bond angle are quite rigid in a PVDF polymer molecule, the vibrational potential and bending potential have little influence on chain conformation [18]. We modify the model by assuming bond lengths and bond angles are fixed (with vibrational and bending energy excluded), and their equilibrium values are listed in Table 1.

With these simplifications, the total conformational energy of a molecule is composed of three types of interactions, including electrostatic dipolar V_{el}, van der Waals V_{vdW}, and torsional potential V_{tor}, respectively, given by

$$V_{\mathrm{el}} = \sum_{i>j} \frac{q_i q_j}{\varepsilon r_{ij}} \tag{1}$$

$$V_{\mathrm{vdW}} = \sum_{i>j} A_{ij} \exp(-B_{ij} r_{ij}) - \frac{C_{ij}}{r_{ij}^6} \tag{2}$$

$$V_{\mathrm{tor}} = \sum_{i,j,k,l} \sum_{n} \frac{1}{2} K(n)_{ijkl} [1 - \cos(n\phi_{ijkl})] \tag{3}$$

where q_i is the partial atomic charge on atom i, ε is the dielectric constant, and r_{ij} is the distance between atoms i and j. A_{ij}, B_{ij} and C_{ij} are Buckingham exponential parameters for van der Waals interactions, ϕ is the torsional angle formed by bonded atoms i, j, k and l. V_{el} and V_{vdW} apply to all nonbonded atom pairs that are separated by at least three bonds, and the 1–4 interactions

Table 1 Equilibrium bond lengths, bond angles and partial charges employed in our MC simulations

Bond lengths (Å)		Bond angles (deg)		Partial atomic charges	
C–C	1.534	F–C_F–F	105.27	C_H	−0.5202
C–H	1.085	F–C_F–C_H	107.74	C_F	0.6120
C–F	1.357	C_H–C_F–C_H	118.24	H	0.1807
		H–C_H–H	109.27	F	−0.2266
		H–C_H–C_F	108.45		
		C_F–C_H–C_F	118.24		

(atoms separated by three bonds) are not scaled specially. The parameters for the above potentials are obtained from the same force field. Note, that van der Waals interactions and electrostatic interactions account for instantaneous induced dipole–dipole interactions and permanent dipole–dipole interactions in a molecule, respectively.

In addition to equilibrium bond lengths and bond angles, Table 1 also summarizes the partial atomic charges of different atoms for the model. In the calculations, we choose the same partial charge q for the carbons of the same type (i.e. q=−0.5202 for all methylene carbons and 0.6120 for all fluoro-methylene carbons). Each repeated unit (CH_2CF_2) satisfies electroneutrality, and the two chain ends are terminated by –CF_3 (next to –CH_2–) and –CH_3 (next to –CF_2–), respectively. Note, that the large difference of the partial charges between two neighboring carbons indicates that the dipolar interactions within in a PVDF molecule arise from other bonds other than C–F bond alone. To simplify the model further, we neglect the partial charges of one of the three hydrogen (and of fluorine atoms) on chain ends. In fact, we have tested other choices to model chain ends, for example, by incorporating partial charges into the H and F atoms of both ends, but the results are not affected by these variations due to insignificant contribution from chain ends.

In the van der Waals potentials, Byutner and Smith made use of exponential functions, but noticeably, these exponential functions produce unphysical energy wells at very small distances. Figure 1 plots the van der Waals potentials between two nonbonded carbons, in which a well emerges for r_{ij}<1.2 Å. Such an unphysical potential well is also observed for the van der Waals potential between other atoms. Although the chance of crossing the barrier into this energy well is essentially zero in the molecular dynamics simulations by Byutner and Smith [8], this unphysical well can be frequently sampled in our MC simulations, and results in the abnormal collapse of chain conformation. To rectify this problem, we impose a cut-off distance on each van der Waals potential, slightly to the right of the peak of the corresponding original van der Waals potential, to prevent two atoms from falling into this regime. In Table 2, we summarize the cut-off distances of the van der Waals potentials between different atoms for our modified model. To validate these modifications, we test different cut-off distances (by up to ±10% of the chosen cut-off values), and the simulation results are independent of our choices.

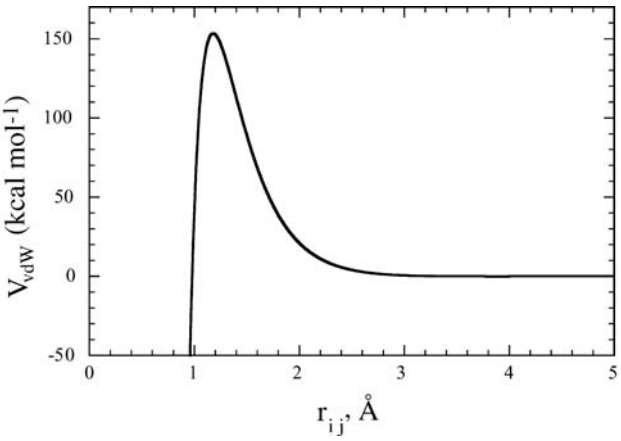

Fig. 1 Potential function of the original van der Waals interaction between two nonbonded carbon atoms

Monte Carlo simulation

In this work, we conduct simulations using the Monte Carlo (MC) method to investigate the conformational transition between distinct globular and coiled conformational states, as well as the effective attractive interactions induced by dipolar interactions (concluded from our results). To this end, MC may be more feasible to prevent a chain molecule from being trapped in the local energy minimum of a collapsed conformation because more drastic moves can be employed to force chain molecules to escape from the meta-stable energy wells.

In the MC simulations, we relax chain conformation by changing torsional angles on the PVDF backbone. For each simulation step, we randomly select a C–C bond on the PVDF backbone and choose a new torsional angle randomly between $-\pi$ and π. Such a simulation move is the same as that used in the RMMC algorithm [19, 20, 21]. In the RMMC algorithm, a cut-off is introduced in the calculation of energy, and only those interactions within a few monomers near the bond chosen for rotation are considered. However, in our simulations, we consider the energy of the entire molecule with all interactions, because we intend to incorporate both short-range and

Table 2 Cut-off distances for the VdW potentials between different atomic species in MC simulations

Atom pair	Cut-off distances (Å)	Atom pair	Cut-off distances (Å)
(C, C)	1.2	(H, H)	1.0
(C, H)	1.2	(H, F)	1.2
(C, F)	1.5	(F, F)	1.5

long-range interactions into the model. As in the RMMC algorithm, we accept a move based on the probability P_{accept} of the Metropolis criterion, given by

$$P_{\text{accept}} = \min(1, -(E_{\text{new}} - E_{\text{old}})/k_{\text{B}}T) \quad (4)$$

where E_{new} and E_{old} are the energies of the entire molecule for the new and the old conformation, k_{B} is the Boltzmann constant and T is the temperature.

In the simulations, the chain length is varied from M=4 to 20 where M is the number of repeated units (monomers) of a PVDF molecule to investigate the chain-length dependent conformational behaviors. The chosen chain lengths are short compared to those in industrial PVDF materials, but these chain lengths fall into the range of recent experimental and theoretical interests for short chain peptides and polymers [2, 3, 4, 5]. Moreover, the temperature T is varied between 200 K and 500 K, and the dielectric constant of the medium is chosen in the range between ε=1 and 8. Note, that in the work of Byutner and Smith [8], all atoms are explicitly incorporated in the simulation of bulk PVDF materials and ε is chosen to be 1. In our simulations, however, dielectric constant plays two roles: (1) to adjust the strength of electrostatic interactions; (2) to represent the condensed phase environment (i.e., dipolar interactions mediated by the medium). For example, for ε=1, dipolar interactions reach the maximum strength for this model system, and ε=8 approximates the value of amorphous PVDF material. In our calculations, the chosen temperatures and dielectric constants are based on experimentally relevant conditions [22].

In the simulations, we first compute the chain conformation characterized by mean chain size, i.e. mean squared end-to-end distance $\langle R^2 \rangle$ of the carbon backbone of a PVDF molecule (between the two end carbon atoms). A total of 1×10^8 moves are conducted for each simulation, and we skip $2M$ moves to allow the molecule to relax before a new equilibrated conformation is sampled. Namely, a total of $5\times10^7/M$ equilibrated conformations are used to calculate simulated mean properties. To test the simulations, we calculate the cumulative $\langle R^2 \rangle$ with respect to Monte Carlo steps τ, as well as the autocorrelation function of normalized end-to-end vector (the vector $r_{\mathbf{ee}}$ between the two end carbons) $C(\tau)$, defined as

$$C(\tau) = \langle r_{ee}(\tau) \cdot r_{ee}(0) \rangle = \frac{1}{\tau_{\max}} \sum_{\tau_0=1}^{\tau_{\max}} r_{ee}(\tau + \tau_0) \cdot r_{ee}(\tau_0) \quad (5)$$

where $\tau_{\max}$ is the number of time steps (simulation moves in MC) of ensemble average of each time origins [23].

In addition to chain conformation, we monitor the distribution of the instantaneous end-to-end distance r_{ee} (between the two end carbon atoms), which reads

$$P(r_{ee}) = H(r_{ee})/\Delta r_{ee} \quad (6)$$

where $H(r_{\text{ee}})$ is the histogram obtained from simulations and Δr_{ee} is the grid size of histogram. We set Δr_{ee}=0.025×M Å in the calculations. To better understand the effect of interaction energies on chain conformation, we expand the single variable distribution function $P(r_{\text{ee}})$ to a two-variable distribution function of instantaneous end-to-end distance and energy, given by

$$P(r_{ee}, E) = H(r_{ee}, E)/\Delta r_{ee}/\Delta E \quad (7)$$

where ΔE is set to be 0.1 kcal mol^{-1}.

Results and discussion

Test of algorithms

We first test the performance of our simulation algorithm by checking the cumulative average of mean squared end-to-end distance and the autocorrelation function of the end-to-end vectors, as shown in Fig. 2. Figure 2a plots the cumulative mean squared end-to-end distance as the number of simulation moves (i.e., time τ in Eq. 5) for M=8 and 15 for ε=8, and for comparison, we also plot M=15 and ε=1. We obtain good convergence for all the cases (different temperatures and dielectric constants), even for the longer chain (M=15), except at the very low temperature (200 K). Moreover, we perform temperature quenching and annealing (at a rate of 20 K) simulations, and the results are independent of the simulation procedures. Figure 2b displays the autocorrelation function $C(\tau)$ (from Eq. 5) for the same parameters as in Fig. 2a. Again we find the end-to-end vectors are randomized in a sufficiently short time period except for the long chain case (M=15) at the low temperature (200 K). Note, that we also have conducted tests for the relaxation of the middle segments of a chain molecule, and obtain fast relaxation, as end-to-end vectors, for T greater than 200 K and for different dielectric constants and chain lengths (data not shown). In other words, the algorithm offers reasonable performance for chain length up to M=15 and temperature down to near 200 K. (Note that for each simulation we conduct 1×10^8 moves to achieve good statistics.)

Effects of the strength of interactions on mean chain size

In the simulations, we initiate our calculations for the two environmental parameters, temperature and dielectric constant, to fine-tune the strength of the overall interactions and to single out the contribution of dipolar interactions, respectively. Figure 3 plots the mean chain size $\langle R^2 \rangle$ as a function of temperature for different chain lengths, M=8 and 12, and for two dielectric constants, ε=1 and 8, as marked. In all cases, chain size grows with increasing temperature, which suggests that the overall intramolecular interactions of a PVDF chain molecule are attractive. For a given chain length, the chain dimension tends to be more contracted at smaller dielectric constant, which may be attributed to the increased strength of attractive intramolecular dipolar interactions.

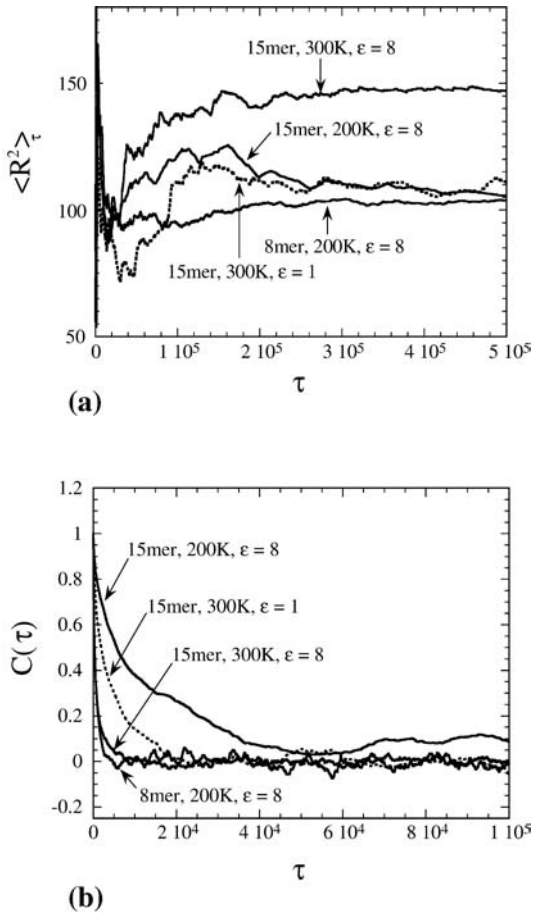

Fig. 2a,b Plots of cumulative $\langle R^2 \rangle$ against number of simulation moves τ for 8-mer and 15-mer for different temperatures and ε=8, (and for 15-mer and ε=1 for comparison), as marked, in **a**, and autocorrelation function $C(\tau)$ (defined in Eq. 4) in **b** for the same parameters as in **a**

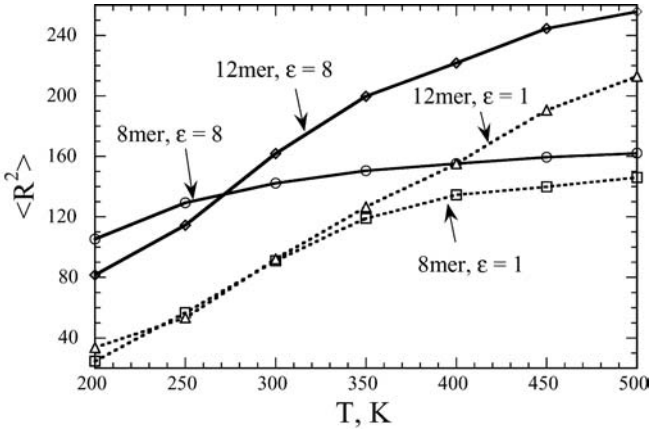

Fig. 3 Variation of $\langle R^2 \rangle$ with temperature for different dielectric constants ε=1 and 8, denoted by dotted and solid lines, respectively, and for different chain lengths M=8 and 12, as marked. Lines are meant for eye guidance

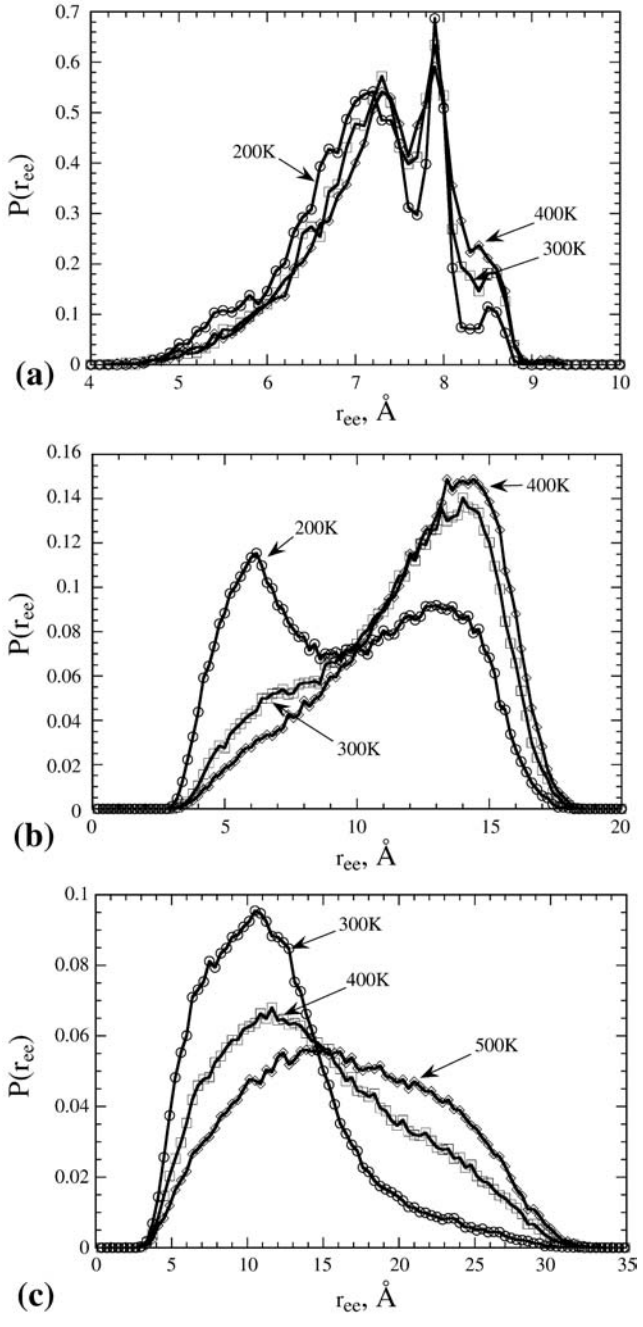

Fig. 4a–c Chain size distribution for different chain lengths M=4 in **a**, M=8 in **b**, and M=12 in **c** for ε=8 for different temperatures, as marked. Lines are meant for eye guidance

Effect of the strength of interactions on chain size distribution

To elucidate the effects of the strength of overall interactions on conformational transition, we compute the size distribution $P(r_{ee})$ for different temperatures. Figure 4 plots $P(r_{ee})$ for chain lengths M=4 in Fig. 4a, M=8 in Fig. 4b and M=15 in Fig. 4c, for dielectric constant ε=8 and for different temperatures (ranging from 200 K to 400 K for M=4 and 8, and from 300 K to 500 K

for M=15). When the chain length is short (M=4 in Fig. 4a, the chain molecule displays some features similar to very short conformers, i.e., the $P(r_{ee})$ consists of multiple peaks and many small bumps for each peak (by noting that simulation errors are about the size of symbols). These distinct peaks and bumps, particularly for the lowest temperature in Fig. 4a (T=200 K), can be attributed to the distinct energy difference for different conformations, as seen for very short conformers (M<4). Note, that multiple peaks become more pronounced below T=200 K (data not shown). When the temperature is increased from 200 K up to 400 K, the small bumps for each peak diminish, and the third peak near r_{ee}=8.4 Å at 200 K becomes a shoulder of the peak located at r_{ee}=7.9 Å at 400 K. Namely, the $P(r_{ee})$ is in the form of a bimodal-like distribution (with two primary peaks). As chain length is increased to M=8, the distribution of $P(r_{ee})$ can be a single-modal and bimodal function, but the distribution is quite smooth without small bumps present for all temperatures. At the low enough temperature, $P(r_{ee})$ is a bimodal function, and this bimodal distribution persists at the lowest temperature in our simulations for ε=8. In the bimodal distribution, the two peaks emerge at near r_{ee}=6.2 Å and 13.6 Å, corresponding to the coexistent globular and coiled state for chain conformations. When the temperature is increased to T=300 K, the peak near $r_{ee}\approx$6.2 Å diminishes, and $P(r_{ee})$ becomes a single-modal function with a shoulder present near $r_{ee}\approx$6.7 Å. When the temperature is increased to T=400 K, the $P(r_{ee})$ shows a single peak located near 13.8 Å, due to the predominant coiled state. The transformation of bimodal distribution to single-modal distribution is an indication of discontinuous globule-coil conformational transition, as has been shown in previous theoretical [15, 16, 17] and experimental [13, 14] studies in the literature. Thermodynamically, the two conformational states correspond to one metastable and one stable state, depending on their free energies. At the transition temperature, the free energy of the two states is the same. Furthermore, as the chain length is increased to M=15, the $P(r_{ee})$ is a single-modal distribution function for all simulated temperatures. The peak position moves continuously toward larger r_{ee} as the temperature is increased, suggesting a continuous conformational transition from globular state to coiled state.

In Fig. 5, we plot the chain size distribution function for M=8 and ε=1 for different temperatures, as marked. In contrast to Fig. 4b (for M=8 and ε=8), the distribution function also shows a bimodal profile, but the statistical weight for the globular state becomes greater. When the temperature is high (around 500 K), we observe single-modal distribution, and chain tends to be in the more stretched coil state. For a lower temperature, the distribution becomes bimodal (with coexistent globular and coiled conformations). As the temperature is decreased further, the bimodal behavior diminishes, and eventually, the single peak emerges, corresponding to globular conformational state. The results indicate that dipolar interactions induce conformational contraction, and favors globular conformations.

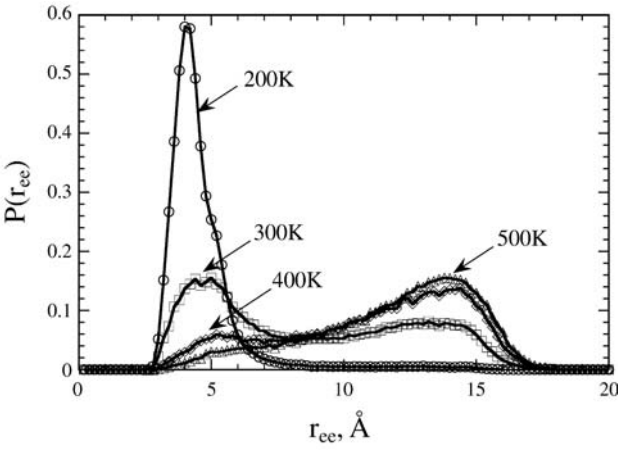

Fig. 5 Chain size distribution for chain length M=8 and ε=1 for different temperatures, as marked. Lines are meant for eye guidance

Chain-length dependence of discontinuous globule-coil conformational transition

The phase behavior of a thermodynamic system can be obtained from its free energy. Although the free energy is not calculated directly in our simulations, the simulated distribution function $P(r_{ee})$ is related to the free energy (proportional to $-\ln[P(r_{ee})]$) as a function of chain size. In the following, we define the transition temperature, from one conformational state to the other, as the temperature at which the two peaks of the bimodal distribution have approximately the same height. In Fig. 6 we plot $P(r_{ee})$ for chain length M=8, 10 and 12 for ε=8 in Fig. 6a and for ε=1 in Fig. 6b when the two peak heights of the bimodal distribution are about the same. Figure 6a shows that as the chain length is increased, the transition occurs at higher temperatures and the bimodal profile becomes less pronounced. For long enough chains, the bimodal behavior of $P(r_{ee})$ diminishes completely and becomes a single-modal distribution, as seen in Fig. 4c. In Fig. 6b, we find that decrease of dielectric constant results in an increase of transition temperature, suggesting that the chain molecule is in favor of the globular conformational state as dipolar interactions are increased.

Effects of dipolar interactions on chain size distribution and conformational transition

To rationalize the influence of dipolar interactions, we vary the dielectric constant to adjust the interaction strength arising from polar bonds. Figure 7 plots the distribution function $P(r_{ee})$ for M=8 and T=300 K in Fig. 7a and for M=12 and T=400 K in Fig. 7b for different dielectric constants, as marked. Note, that for dielectric

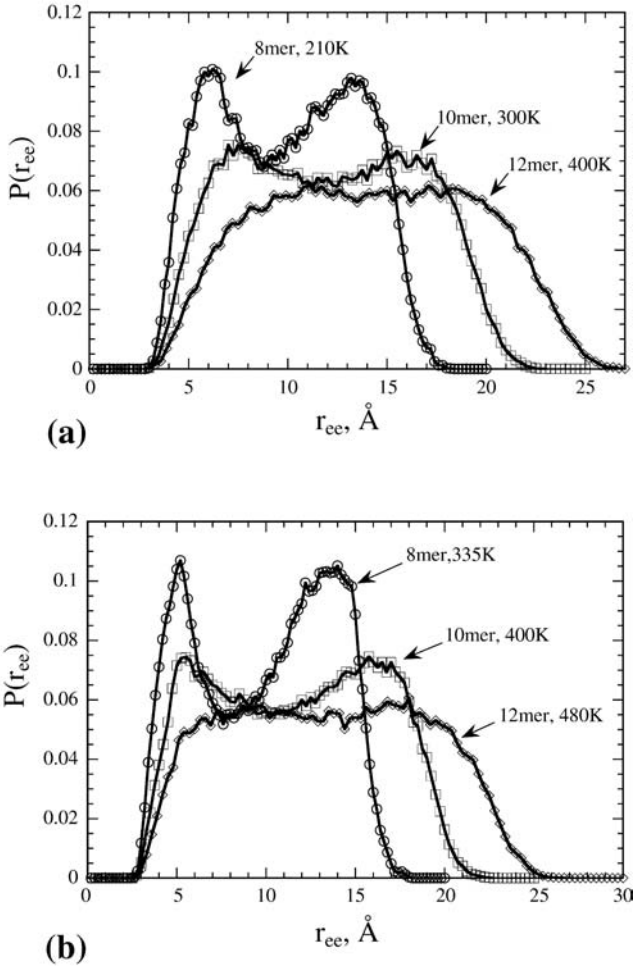

Fig. 6a,b Chain size distribution near the transition temperature for different chain lengths, as marked, for ε=8 in **a** and ε=1 in **b**. Lines are meant for eye guidance

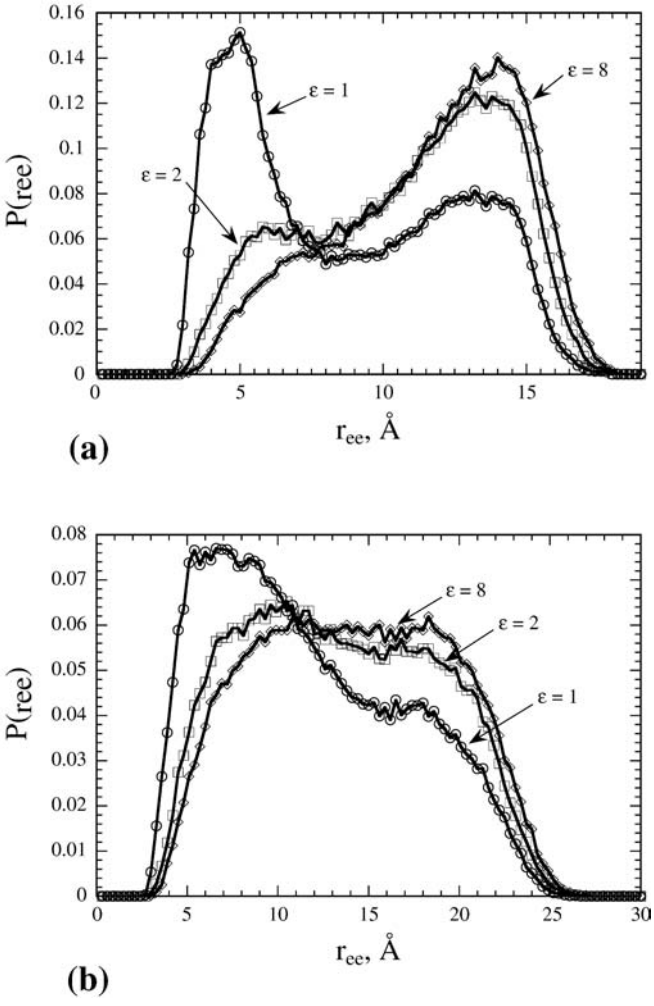

Fig. 7a,b Chain size distribution for M=8 and T=300 K in **a** and for M=12 and T=400 K in **b** for different dielectric constants, as marked. Lines are meant for eye guidance

constant ε>8, we find the $P(r_{ee})$ is almost identical to that of ε=8; namely the contribution from dipolar interaction becomes negligible at this temperature. In Fig. 7a, for ε=8, there is only one peak observed in $P(r_{ee})$, corresponding to more stretched coiled chain conformations. As the dielectric constant is decreased, the $P(r_{ee})$ becomes bimodal, indicating that the collapsed globular conformations coexist with the more stretched coiled conformations. In contrast to ε=2, the statistical weight of globular state for ε=1 increases significantly because of the stronger dipolar interactions for the smaller dielectric constant. In Fig. 7b, we observe similar features for the longer chain M=12 as the dielectric constant is varied. These results show that dipolar interactions induce chain contraction, and favor more compact globular structures. Increase of dielectric constant, indeed, reduces the contribution from dipolar interactions, and when the dielectric constant is increased to 8, dipolar interactions are greatly reduced with less contribution on the chain conformations. (Note that the observed bimodal behavior also occurs when the monomers interact through van der Waals and torsional interactions alone without dipolar interactions.) From the results of different dielectric constants, we may argue that dipolar interactions enhance the attractive part of total interactions and collapse chain conformation further.

Schematic phase diagrams

We summarize the observed conformational behavior in terms of schematic phase diagrams as a function of temperature and chain length, as shown in Fig. 8 for ε=8 in Fig. 8a and ε=1 in Fig. 8b. The phase diagrams can be divided roughly into three regimes, including short chain, intermediate chain and long chain. (Note that the shaded areas stand for the transition from one regime to the other.) For short chains and long chains, $P(r_{ee})$ exhibits multiple peaks and single peak, respectively. For the intermediate chain length, the dividing lines, denoted by dashed lines, indicate that the transition temperature of

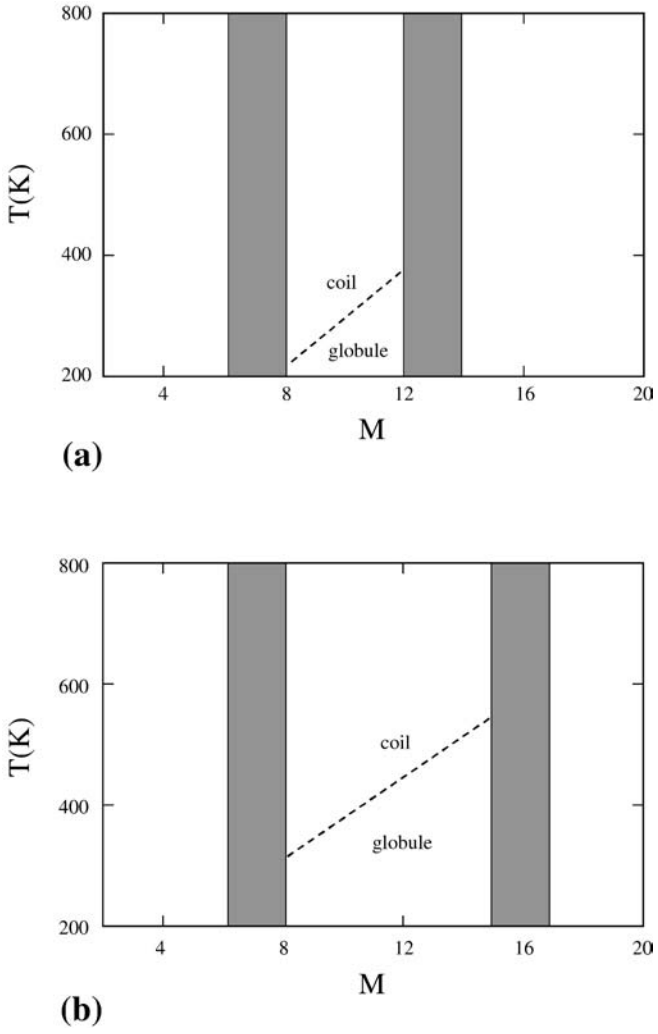

Fig. 8a,b Schematic phase diagrams for ε=8 in **a** and ε=1 in **b**; the transition temperature of discrete conformational transition denoted by dotted curves

the two conformational states. Actually, these findings are analogous to the electronic orbital energy observed in quantum chemistry. When the number of atoms in a molecule increases, such as in conjugated chain molecules, the energy levels can be in the form of discrete states, band gaps or continuous energy states, depending on chain lengths [3, 24].

Compared to ε=8, we find that the general features of the phase diagram remain similar for ε=1, and the boundary to separate short chains from intermediate chain length is roughly the same. However, the boundary to divide the intermediate chain length and long chain tends to move toward larger chain lengths. Also, for a given chain length, the transition temperature increases when ε is decreased to 1.

These results may be understood from the perspectives of chain flexibility and effective intramolecular attractive interactions. As pointed out by Grosberg and Khokhlov [25], the discontinuous conformational transition, as seen for the intermediate chain lengths of PVDF molecules, is sensitive to chain stiffness. For smaller chain lengths, the effective intramolecular attractions are not sufficient to contract a stiff short PVDF chain. For intermediate chain lengths, the chain becomes slightly more flexible and can be deformed in the presence of attractive interactions. As a result, the chain molecule can either elongate or contract, with different mechanisms to lower the conformational free energy. Namely, the elongated chain molecule gains conformational entropy, and the contracted chain molecule gains internal energy. For longer chains, the chain molecule is effectively more flexible and gives rise to more different conformations; the density states of conformational energy and conformational transition become continuous. From the standpoint of energy, the strong dipolar interactions (at smaller dielectric constants) induce more attraction to stabilize globular conformations at higher temperatures, and counterbalance the large conformational entropy for longer chains to maintain the distinct globular (energy driven) and coiled (entropy driven) states.

More detailed energetic analysis

The PVDF molecule of intermediate chain lengths displays distinct conformational states, and will be useful to discern the effects of different molecular interactions on chain conformations. We first expand the chain size distribution $P(r_{ee})$ to a function of two variables $P(r_{ee}, E)$, instantaneous chain size (r_{ee}) and energy (E), because such a function depicts the correlation between chain size and interaction energy, and can be used to verify the presence of discrete conformational transition. In the simulations, E can be the energy of total interactions or individual interaction terms. Figure 9 displays the contour plots of $P(r_{ee}, E_{total})$ for total energy in Fig. 9a, $P(r_{ee}, E_{el})$ for electrostatic energy in Fig. 9b, $P(r_{ee}, E_{VdW})$ for van der Waals energy in Fig. 9c, and $P(r_{ee}, E_{tor})$ for torsional energy in Fig. 9d for 8-mer for ε=8 and T=200 K. Note, that the reported energies are relative to the energy of the totally stretched zig-zag conformation. The chosen parameters for the calculations in Fig. 9 are the same as the curve for T=200 K in Fig. 4b. In Fig. 9a, $P(r_{ee}, E_{total})$ has the two distinct peaks of approximately the same statistical weight, and the energy difference between two peaks is about 2 kcal mol^{-1}. These two peaks correspond to the coiled conformational state of higher energies and the globular conformational state of lower energies. In Fig. 9b, the electrostatic energy difference between the two peaks of $P(r_{ee}, E_{el})$ is rather small (only about 0.3 kcal mol^{-1}). Meanwhile, the torsional energy difference between two conformational states is negligible, as shown in Fig. 9d. However, in Fig. 9c, the van der Waals energy results in a much greater energy difference between two peaks (about 1.7 kcal mol^{-1}), which accounts for the primary energy difference between two conformational states. From the contour plots of different types of energy, we notice that the energy levels of two

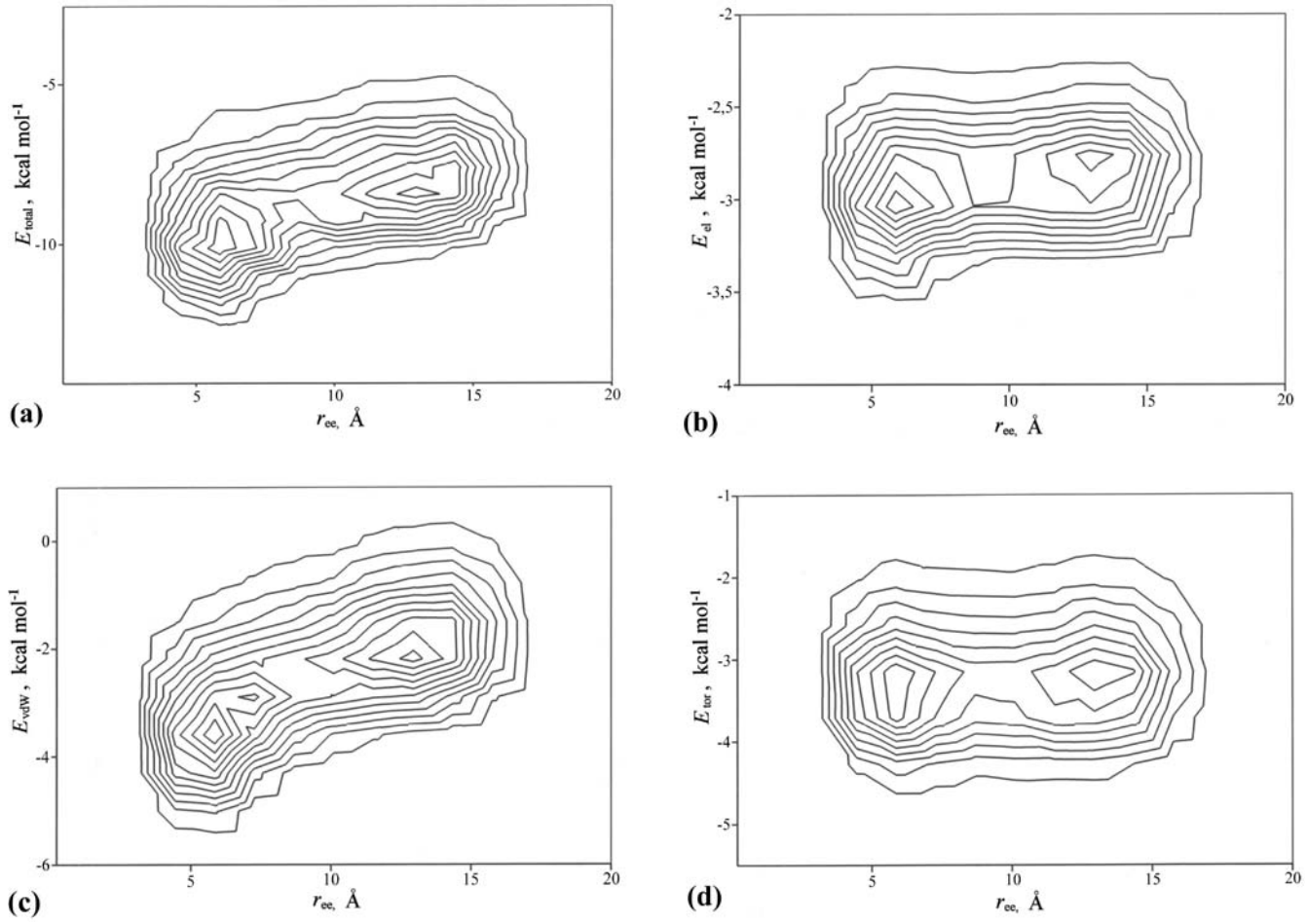

Fig. 9a–d Contour plots for $P(r_{ee}, E_{total})$ for total energy in **a**, $P(r_{ee}, E_{el})$ for electrostatic energy in **b**, $P(r_{ee}, E_{vdw})$ for van der Waals energy in **c**, and $P(r_{ee}, E_{tor})$ for torsional energy in **d** for 8-mer for ε=8 and T=200 K

distinct conformational states may reveal the nature of interaction potentials. For weak or short-ranged molecular potentials, such as weak dipolar interactions for ε=8 and short-ranged torsional interactions, the two conformational states in the two distinct peaks have a similar potential energy level. For stronger molecular interactions, such as van der Waals interactions, the energy level is significantly different between the two conformational states. Despite the fact that dipolar interactions and van der Waals interactions have comparable length scales, for ε=8, dipolar interactions are screened out significantly, and van der Waals interactions are crucial in governing chain conformations.

Moreover, the contour plot is also helpful to identify the effects of dipolar interactions. Figure 10 displays the contour plots of $P(r_{ee}, E_{total})$ in Fig. 10a and $P(r_{ee}, E_{el})$ in Fig. 10b for 8-mer for T=300 K and ε=1, by noting that the contour plots of van der Waals energy and torsional energy are roughly same as those in Fig. 9. The chosen temperature corresponds to Fig. 7a with distinct bimodal distribution. In Fig. 10, $P(r_{ee}, E_{total})$ and $P(r_{ee}, E_{el})$ show similar features, i.e., the energy levels of the two distinct conformational states are quite different. Unlike Fig. 9, the electrostatic interactions in Fig. 10 have significant contributions to the conformational energy (the energy difference between two conformational states is 1.8 kcal mol^{-1} for electrostatic interactions). Namely, for the smaller dielectric constant ε=1, the globular conformations are substantially stabilized by electrostatic interactions. Meanwhile, the energy difference of van der Waals interactions (or torsional interactions) between the two conformational states is insensitive to the presence of dipolar interactions.

Representative snapshots of chain conformations

In addition to average characteristic properties, we here present a few typical snapshots to illustrate the molecular structure of chain conformational states. For illustration purpose, we report the snapshots obtained from the simulations for M=12 and T=400 K. Figure 11 displays the snapshots (with carbon backbone sketched only for clarity) for globular conformation for ε=8 in Fig. 11a, coiled conformation for ε=8 in Fig. 11b, and the globular conformation for ε=1 in Fig. 11c. Fig. 11a and b

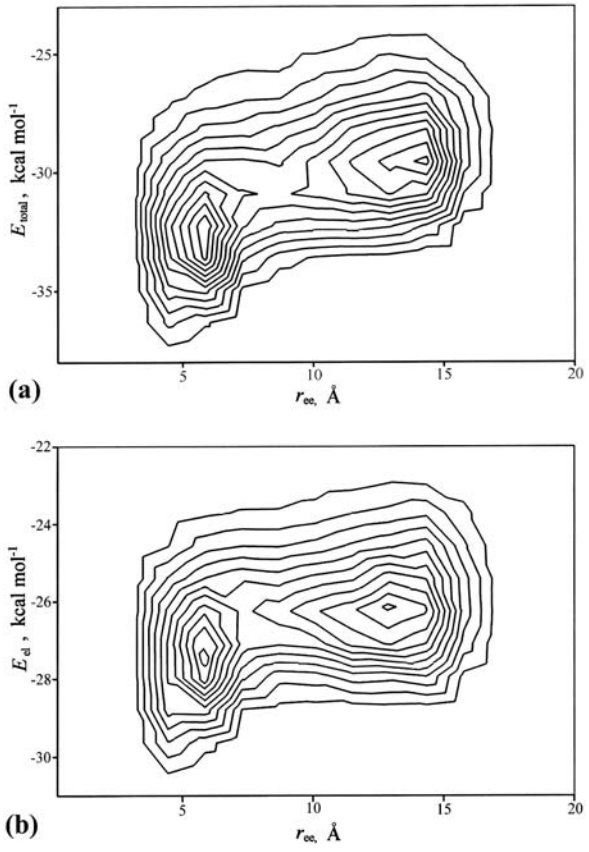

Fig. 10a,b Contour plots of $P(r_{ee}, E_{total})$ in **a** and $P(r_{ee}, E_{el})$ in **b** for 8-mer for T=300 K and ε=1

correspond to the globular and coiled chain conformation in Fig. 7b, in which the chain molecule adopts a partially folded middle segment and a stretched coil, respectively. As for dielectric constant ε=1, the simulated conformations are not very different from those seen for dielectric constant ε=8. However, in the simulations, the hairpin-like structures in globular conformations (with more compact loops than Fig. 11a) are more frequently encountered, as shown in Fig. 11c, due to stronger dipolar interactions.

The PVDF model consists of the general molecular interactions found in many other polymeric molecules, which can serve as a model system to elucidate the conformational behavior for more complex copolymers or biopolymers. To our best knowledge, the chain conformation of single PVDF molecules has not been systematically studied although the molecule may exhibit significant vibrational–circular dichroism signals due to strong polar bonds [26]. Nevertheless, an increase of interest has been devoted to understanding the chain-length dependent single peptide conformation, such as oligomeric N-substituted glycines or "peptoids" reported by Wu et al. through CD spectra [27]. Such a peptide is unique because it is believed that hydrogen bonding is not important for its secondary structure. Their findings suggest that the conformation of these peptides is sensitive to chain length. For example, for very short peptides (5–8 amino acids), the peptide molecules of different chain lengths share similar spectral characteristics, indicating that their conformations are roughly the same. When the chain length of the peptide is increased to

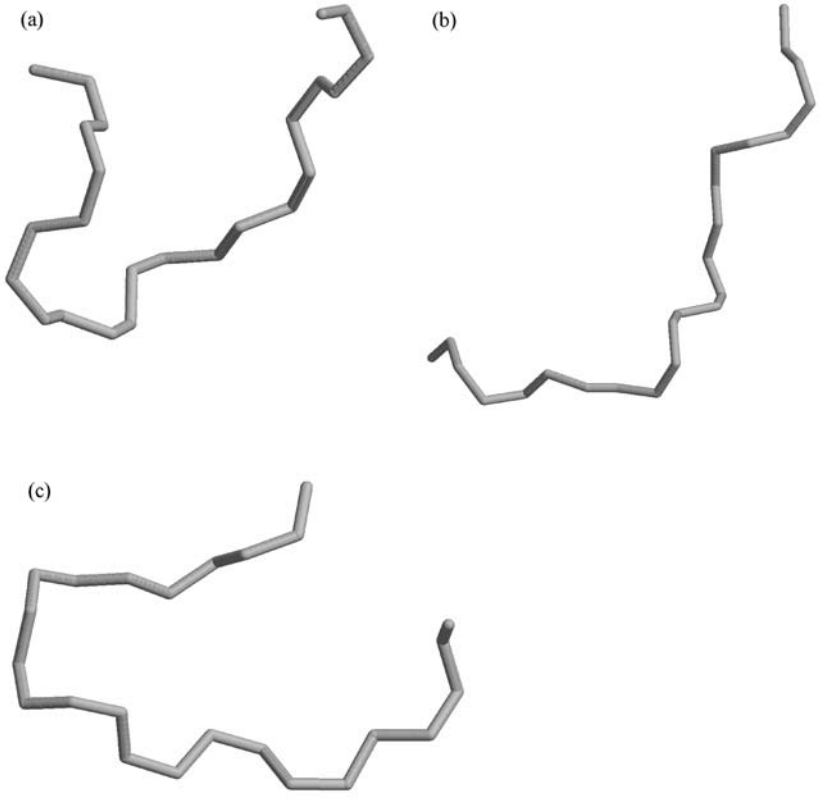

Fig. 11a–c Representative snapshots for the globular conformation for 12-mer at 400 K, ε=8 in **a**, the coiled conformation for ε=8 in **b**, and the globular conformation for ε=1 in **c**, with carbon backbone sketched

the range between 8 and 13 amino acids, the chain conformation is strongly affected by chain length, and these peptides show two major spectral bands of different intensities for these chain lengths. We speculate that the chain-length dependent conformational behavior may be caused by coexistent globular and coiled conformational states (observed within the regime near the discrete globule–coil transition).

Conclusion

We have conducted atomistic Monte Carlo simulations to investigate the conformational behavior of a modified PVDF model in which bond lengths and bond angles are fixed. The simulation is conducted at the single chain level, and the condensed phase environment is treated as a dielectric continuum. Our aim is to investigate the roles of dipolar interactions among different molecular interactions. By varying temperature, we tune the strength of overall interactions altogether, and by varying dielectric constant, we distinguish the contribution of dipolar interactions from other types of interactions.

In the simulations, we investigate mean chain size and chain size distribution. For a given chain length, the mean chain size increases as the temperature is increased. However, the chain size distribution is sensitive to the chain length. For short chains, the distribution function exhibits multiple peaks, even for higher temperatures, consistent with conformer behaviors. For intermediate chain lengths, the chain conformation distribution makes a transition between single-modal distribution and bimodal distribution as the temperature is changed. Such a behavior can be recognized as a discrete conformational transition. To verify the presence of discrete conformational transition further, we compute the distribution as a function of chain size and energy and obtain contour plots of these variables. We identify such a discrete conformational transition from the bimodal distribution in the contour plot. For longer chains, the distribution displays a broad peak and conformational transition becomes continuous.

Polar bonds (C–C, C–H, C–F) induce dipolar interactions that are effectively attractive. We find that as dipolar interactions are increased, mean chain size decreases, and the globular conformational state becomes more pronounced. Meanwhile, the discrete conformational transition for intermediate chain lengths shifts toward higher temperatures and/or longer chain lengths. From the analysis of different types of interaction energy, we find that van der Waals and torsional interactions are responsible for the coexistent conformational states, and the dipolar interactions induced by polar bonds further enhance the attractive part of molecular interactions and the stability of globular states.

In addition to aforementioned chain properties, we also have monitored snapshots for the simulated conformations systematically. The globular conformation is characterized by a folded middle segment, whereas the coiled conformation is much more stretched out. When the strength of dipolar interactions is increased, a hairpin-like structure with more compact loops is more frequently sampled.

We have conducted rigorous tests for the simulation algorithm, and have obtained reasonable convergence for the range of our calculations (above 200 K and around $M \leq 20$). In the future, we will incorporate other algorithms to facilitate the simulations of compact chain conformations, such as the Parallel-Rotation method suggested by Santos et al. [28]. Also, we intend to investigate the conformational behavior at low temperature in search of a single chain crystal structure of a PVDF molecule, many chain systems, as well as the influence of electric fields on the properties of PVDF.

Acknowledgement We acknowledge partial support from the CUNY Collaborative Incentive Award # 92922-00-08 and the support from PSC-CUNY grants # 63355-00-32, # 64379-00-33 and # 65367-00-34 as well as the New York Fine Chemicals Corporation.

References

1. Dill KA (1990) Biochemistry 29:7133–7155
2. Liang H, Chen H (2000) J Chem Phys 113:4469–4471
3. (a) Taylor MP (2001) J Chem Phys 114:6472–6484; (b) Taylor MP (2003) J Chem Phys 118:883–891
4. Katakai R (1977) J Am Chem Soc 99:232–234
5. (a) Neidigh JW, Fesinmeyer RM, Andersen NH (2002) Nat Struct Biol 9:425–430; (b) Gellman SH, Woolfson DN (2002) Nat Struct Biol 9:408–410; (c) Qiu L, Pabit SA, Roitberg AE, Hagen SJ (2002) J Am Chem Soc 124:12952–12953
6. Karasawa N, Goddard III WA (1992) Macromolecules 33:7268–7281
7. Byutner OG, Smith GD (1999) Macromolecules 32:8376–8382
8. Byutner OG, Smith GD (2000) Macromolecules 33:4264–4270
9. Binder K (1995) Monte Carlo and molecular dynamics simulations in polymer sciences. Oxford University Press, Oxford
10. Cao J, Berne BJ (1989) J Chem Phys 92:1980–1985
11. Borkovec M, Berne BJ (1987) J Chem Phys 86:2444–2446
12. Shew C-Y, Mills P (1993) J Phys Chem 97:13824–13830
13. Yamasaki Y, Yoshikawa K (1997) J Am Chem Soc 119:10573–10578
14. Yamasaki Y, Yoshikawa K (2001) Adv Drug Delivery Rev 52:235–244
15. Noguchi H, Yoshikawa K (1998) J Chem Phys 109:5070–5077
16. Shew C-Y, Yethiraj A (1999) J Chem Phys 110:676–681
17. Takagi S, Tsumoto K, Yoshikawa K (2001) J Chem Phys 114:6942–6949
18. Chang G, Guida WC, Still WC (1989) J Am Chem Soc 111:4379–4386
19. Honeycutt JD (1998) Comput Theor Polym Sci 8:1–8
20. Bicerano J (1998) Comput Theor Polym Sci 8:9–14
21. Bicerano J, Brewbaker JL, Chamberlin TA (1998) Comput Theor Polym Sci 8:15–20
22. Bicerano J (1996) Predictions of polymer properties, 2nd edn. Marcel Dekker, New York
23. Allen MP, Tildesley DJ (1987) Computer simulation of liquids. Oxford University Press, Oxford
24. Calvo F, Doye JPK, Wales DJ (2002) J Chem Phys 116:2642–2649
25. Grosberg AY, Khokhlov AR (1994) Statistical physics of macromolecules. American Institute of Physics, New York
26. Xie P, Zhou Q, Diem M (1995) J Am Chem Soc 117:9502–9508
27. Wu CW, Sanborn TJ, Zuckerman RN, Barron AE (2001) J Am Chem Soc 123:2958–2963
28. Santos S, Suter UW, Müller M, Nievergelt J (2001) J Chem Phys 114:9772–9779